

## A global three-dimensional model analysis of the atmospheric budgets of HCN and CH<sub>3</sub>CN: Constraints from aircraft and ground measurements

Qinbin Li,<sup>1</sup> Daniel J. Jacob,<sup>1</sup> Robert M. Yantosca,<sup>1</sup> Colette L. Heald,<sup>1</sup> Hanwant B. Singh,<sup>2</sup> Makoto Koike,<sup>3</sup> Yongjing Zhao,<sup>4</sup> Glen W. Sachse,<sup>5</sup> and David G. Streets<sup>6</sup>

Received 24 October 2002; revised 4 March 2003; accepted 9 April 2003; published 18 October 2003.

[1] We construct global atmospheric budgets of HCN and CH<sub>3</sub>CN through a three-dimensional (3-D) model simulation of the HCN-CH<sub>3</sub>CN-CO system constrained and evaluated with aircraft observations from the Transport and Chemical Evolution Over the Pacific (TRACE-P) mission over the NW Pacific in February–April 2001. Observed background vertical gradients of HCN and CH<sub>3</sub>CN imply a dominant ocean sink for both gases, with deposition velocity of 0.13 cm s<sup>-1</sup> for both and saturation ratios of 0.79 for HCN and 0.88 for CH<sub>3</sub>CN. Observations for both gases in the free troposphere imply a dominant source from biomass burning. Enhancement of HCN observed in Chinese urban plumes is attributed tentatively to residential coal burning. Biomass burning and residential coal burning emission ratios relative to CO of 0.27% and 1.6%, respectively, for HCN, and of 0.20% and 0.25%, respectively, for CH<sub>3</sub>CN, are consistent with observations in biomass burning and Chinese urban plumes. They provide the best model simulation of the ensemble of TRACE-P observations including vertical profiles and HCN-CH<sub>3</sub>CN-CO correlations. They also allow successful simulation of the long-term observations of HCN columns at sites in the Northern Hemisphere, and of the CH<sub>3</sub>CN vertical distribution observed over the northern Indian Ocean. Global biomass burning and Asian residential coal burning sources in the model are 0.63 and 0.2 Tg N yr<sup>-1</sup>, respectively, for HCN and 0.47 and 0.03 Tg N yr<sup>-1</sup>, respectively, for CH<sub>3</sub>CN. Ocean uptake is the dominant sink for both gases, with oxidation by OH representing an additional minor sink. The resulting tropospheric lifetimes are 5.3 months for HCN and 5.8 months for CH<sub>3</sub>CN. The model predicts very low HCN and CH<sub>3</sub>CN concentrations at high southern latitudes, reflecting the assumption of a uniform saturation ratio for ocean uptake; observations in that region are needed. In the free troposphere, the dominance of biomass burning sources (70–85% for HCN and 90–95% for CH<sub>3</sub>CN) implies that both gases can be used as biomass burning tracers. In the boundary layer, CH<sub>3</sub>CN appears to be a better biomass burning tracer. More work is needed to identify the origin of the Chinese urban source of HCN. *INDEX TERMS*: 0312 Atmospheric Composition and Structure: Air/sea constituent fluxes (3339, 4504); 0322 Atmospheric Composition and Structure: Constituent sources and sinks; 0345 Atmospheric Composition and Structure: Pollution—urban and regional (0305); 0365 Atmospheric Composition and Structure: Troposphere—composition and chemistry; 0368 Atmospheric Composition and Structure: Troposphere—constituent transport and chemistry; *KEYWORDS*: biomass burning, pollution, nitriles, ocean uptake

**Citation:** Li, Q., D. J. Jacob, R. M. Yantosca, C. L. Heald, H. B. Singh, M. Koike, Y. Zhao, G. W. Sachse, and D. G. Streets, A global three-dimensional model analysis of the atmospheric budgets of HCN and CH<sub>3</sub>CN: Constraints from aircraft and ground measurements, *J. Geophys. Res.*, 108(D21), 8827, doi:10.1029/2002JD003075, 2003.

<sup>1</sup>Department of Earth and Planetary Sciences and Division of Engineering and Applied Sciences, Harvard University, Cambridge, Massachusetts, USA.

<sup>2</sup>NASA Ames Research Center, Moffett Field, California, USA.

<sup>3</sup>Department of Earth and Planetary Science, University of Tokyo, Tokyo, Japan.

<sup>4</sup>Department of Mechanical and Aeronautical Engineering, University of California, Davis, California, USA.

<sup>5</sup>NASA Langley Research Center, Hampton, Virginia, USA.

<sup>6</sup>Argonne National Laboratory, Argonne, Illinois, USA.

## 1. Introduction

[2] Hydrogen cyanide (HCN) and methyl cyanide (CH<sub>3</sub>CN, also called acetonitrile) are atmospheric tracers of biomass burning [Lobert *et al.*, 1990; Holzinger *et al.*, 1999] and could play a nonnegligible role in the nitrogen cycle [Li *et al.*, 2000]. Ocean uptake has been hypothesized as their dominant sink, with corresponding lifetimes of a few months [Hamm and Warneck, 1990; Li *et al.*, 2000]. However, their atmospheric budgets are still poorly understood. We use here a global three-dimensional (3-D) model analysis of HCN and CH<sub>3</sub>CN observations in Asian outflow from the Transport and Chemical Evolution Over the Pacific (TRACE-P) aircraft mission over the NW Pacific [Singh *et al.*, 2003] to improve the constraints on the sources and sinks of these two gases. The TRACE-P data represent the first in situ measurements for HCN in the troposphere, and one of the first for CH<sub>3</sub>CN. Previous data for HCN are from remote sensing of the total column at several sites around the world [Mahieu *et al.*, 1995, 1997; Rinsland *et al.*, 1999, 2000, 2001, 2002; Zhao *et al.*, 2000, 2002]. Previous in situ measurements of CH<sub>3</sub>CN have been made over the Indian Ocean [de Laat *et al.*, 2001] and over the Amazon [Williams *et al.*, 2001].

[3] It is well established from laboratory and field experiments that biomass burning is a major source for both HCN (0.1–3.2 m Tg N yr<sup>-1</sup>) and CH<sub>3</sub>CN (0.2–1.1 Tg N yr<sup>-1</sup>) (Table 1). It is also well established that sources from automobile exhaust and industrial processes are negligible in comparison [Lobert *et al.*, 1991; Bange and Williams, 2000; Holzinger *et al.*, 2001]. A recent field experiment indicates no emission of HCN from domestic biofuels [Bertschi *et al.*, 2003]. Atmospheric sinks of HCN and CH<sub>3</sub>CN from reaction with OH and O (<sup>1</sup>D), photolysis, and scavenging by precipitation yield lifetimes of a few years [Cicerone and Zellner, 1983; Brasseur *et al.*, 1983]. The solubilities of HCN and CH<sub>3</sub>CN are sufficiently high for ocean uptake to impose atmospheric lifetimes of a few months if loss in the oceanic mixed layer is sufficiently rapid [Hamm and Warneck, 1990; Li *et al.*, 2000]. There is some evidence that HCN and CH<sub>3</sub>CN are consumed biologically in the ocean [Singh *et al.*, 2003]. Li *et al.* [2000] showed in a global 3-D model study that the observed seasonal variation of the HCN column in different regions of the world is consistent with a scenario where biomass burning provides the main source and ocean uptake provides the main sink. They inferred a global HCN biomass burning source of 1.4–2.9 m Tg N yr<sup>-1</sup>, and an oceanic saturation ratio of 0.83 or less. Observed vertical gradients of HCN and CH<sub>3</sub>CN in remote marine air in TRACE-P confirm the importance of the ocean sink [Singh *et al.*, 2003].

[4] The TRACE-P mission was conducted in February–April 2001 over the NW Pacific to study the transport and chemical evolution of Asian outflow over the Pacific [Jacob *et al.*, 2003]. It used two NASA aircraft, a DC-8 and a P-3B, operating out of Hong Kong and Japan, and with additional transit flights and sorties over the North Pacific. Biomass burning in SE Asia is an important component of Asian outflow in spring [Liu *et al.*, 1999; Chan *et al.*, 2000; Bey *et al.*, 2001b]. During TRACE-P, Asian biomass burning and anthropogenic sources had contributions of similar magni-

tude to CO concentrations observed in Asian outflow [Liu *et al.*, 2003].

[5] Both HCN and CH<sub>3</sub>CN were measured by gas chromatography aboard the DC-8 aircraft [Singh *et al.*, 2003]. The measurement accuracy was ±25% and the detection limit 30 pptv. Other measurements aboard the DC-8 used in this analysis include CO, perchloroethylene (C<sub>2</sub>Cl<sub>4</sub>), and methyl chloride (CH<sub>3</sub>Cl). CO is a general tracer of combustion, C<sub>2</sub>Cl<sub>4</sub> (a synthetic organic chemical used in dry cleaning) is an anthropogenic pollution tracer, and CH<sub>3</sub>Cl is a biomass burning tracer [Blake *et al.*, 2001]. These complementing measurements can be used to place constraints on the sources of HCN and CH<sub>3</sub>CN [Singh *et al.*, 2003]. Some of the results shown by Singh *et al.* [2003] are reproduced here for purpose of comparison to model results. Throughout this paper, model comparisons to observations will use model results sampled along the DC-8 flight paths. All linear regressions are calculated using the reduced major axis (RMA) method, which allows for errors in both variables.

## 2. Model Simulation

[6] We simulate the distributions of HCN, CH<sub>3</sub>CN, and CO observed in TRACE-P with the GEOS-CHEM global 3-D model of tropospheric chemistry. A detailed description of the model is presented by Bey *et al.* [2001a]. We use here GEOS-CHEM version 4.33 (see <http://www-as.harvard.edu/chemistry/trop/geos>). The model is driven by assimilated meteorological fields from the Goddard Earth Observing System (GEOS) of the NASA Data Assimilation Office (DAO). We use meteorological fields for 2000–2001 (GEOS 3) which are provided with 6-hour temporal resolution (3-hour for surface variables and mixed layer depths), 1° × 1° horizontal resolution, and 48 vertical sigma levels. We degrade the horizontal resolution to 2° × 2.5° for application in GEOS-CHEM. The simulations are conducted for a 16-month period (January 2000–April 2001). The first 13 months are used for initialization and we present results for the February–April 2001 TRACE-P period.

[7] Sources and sinks of HCN and CH<sub>3</sub>CN in the model are described in section 3. The CO simulation follows that of Duncan *et al.* [2003] and uses archived OH concentration fields (monthly mean) from a full chemistry simulation [Li *et al.*, 2002] to calculate CO loss. Anthropogenic sources of CO (including contributions from hydrocarbon precursors) are as described by Duncan *et al.* [2003], except for Asia where the Streets *et al.* [2003] inventory is used. Other TRACE-P studies have shown that the domestic fuel source of CO from China is too low in the Streets *et al.* [2003] inventory [Carmichael *et al.*, 2003; Palmer *et al.*, 2003]. For our simulation we double the residential coal source from China, resulting in a total anthropogenic (fossil fuel plus biofuel) source of CO from Asia of 184 Tg CO yr<sup>-1</sup>. Biomass burning sources are as described by Heald *et al.* [2003]. The global biomass burning CO source is 487 Tg CO yr<sup>-1</sup> for 2000, while the global CO sources from fossil fuel and biofuel are 395 and 200 Tg CO yr<sup>-1</sup>, respectively. For the TRACE-P period (February–April 2001), the global biomass burning CO source is 129 Tg CO and about half of that source is in SE Asia.

**Table 1.** Literature Estimates of Global HCN and CH<sub>3</sub>CN Sources (m Tg N yr<sup>-1</sup>)

Biomass Burning	Biofuels	Car Exhaust	Residential Coal	Biogenic	Total	References
<i>HCN</i>						
0.37–1.89					0.2	<i>Cicerone and Zellner</i> [1983] <sup>a</sup>
0.64–3.18		0.04				<i>Lobert et al.</i> [1990] <sup>b</sup>
0.1–0.3						<i>Lobert et al.</i> [1991] <sup>c</sup>
1.4–2.9					1.4–2.9	<i>Holzinger et al.</i> [1999] <sup>d</sup>
0.26	0.21				0.47	<i>Li et al.</i> [2000] <sup>e</sup>
0.7–0.9		<0.02		0.2	1.1	<i>Andreae and Merlet</i> [2001] <sup>f</sup>
0.63			0.2		0.83	<i>Singh et al.</i> [2003] <sup>g</sup> this work <sup>h</sup>
<i>CH<sub>3</sub>CN</i>						
0.27		0.09			0.36	<i>Hamm and Warneck</i> [1990] <sup>i</sup>
0.14–0.75						<i>Lobert et al.</i> [1990] <sup>b</sup>
0.23–1.13						<i>Lobert et al.</i> [1991] <sup>c</sup>
0.14–0.34		0.01				<i>Holzinger et al.</i> [1999, 2001] <sup>d</sup>
0.27	0.17				0.44	<i>Andreae and Merlet</i> [2001] <sup>f</sup>
0.4–0.5		<0.02		0.2	0.7	<i>de Laat et al.</i> [2001] <sup>j</sup>
0.47			0.03		0.5	<i>Singh et al.</i> [2003] <sup>g</sup> this work <sup>h</sup>

<sup>a</sup>Source needed to balance the global sink from oxidation by OH. However, we now know that this reaction makes only a small contribution to the total HCN sink [*Li et al.*, 2000].

<sup>b</sup>Based on emission factors per unit nitrogen of  $2.42 \pm 1.79\%$  for HCN and  $0.95 \pm 0.74\%$  for CH<sub>3</sub>CN measured in laboratory biomass burning experiments and a global biomass burning nitrogen volatilization estimate of  $24\text{--}57\text{ m Tg N yr}^{-1}$  [*Crutzen and Andreae*, 1990].

<sup>c</sup>Based on biomass burning molar emission ratios relative to CO of 1.1% for HCN and 0.25% for CH<sub>3</sub>CN measured in laboratory biomass burning experiments, combined with a global biomass burning CO source estimate of  $480\text{--}860\text{ Tg CO yr}^{-1}$ . No detail of the car exhaust source estimate is given.

<sup>d</sup>Biomass burning sources based on molar emission ratios (relative to CO) of 0.12% for HCN and 0.13% for CH<sub>3</sub>CN measured in a laboratory biomass burning experiment, combined with a global biomass burning CO source estimate of  $210\text{--}550\text{ Tg CO yr}^{-1}$ . The automobile exhaust source of CH<sub>3</sub>CN is based on a measured CH<sub>3</sub>CN molar emission ratio of 0.06 relative to benzene, combined with an emission ratio of 0.6 g benzene per unit fuel (kg C) consumed in traffic [*de Fre et al.*, 1994] and a global fuel consumption estimate of  $2.6 \times 10^3\text{ Tg C yr}^{-1}$  (G. Marland et al., Global, regional, and national CO<sub>2</sub> emission estimates from fossil-fuel burning, hydraulic cement production, and gas flaring: 1751–1995, CDIAC-Database NDP-030/R8, 1998, available at <http://cdiac.esd.ornl.gov/ndps/ndp030.html>).

<sup>e</sup>Source needed to balance the HCN loss derived from the relative seasonal amplitude of the column observations, when fitted in a global model simulation (GEOS-CHEM version 3.4) with biomass burning as the only source and ocean uptake as the dominant sink.

<sup>f</sup>Biomass burning sources based on HCN molar emission ratios relative to CO of 0.05% for savanna and grassland and 0.15% for tropical and extratropical forests and CH<sub>3</sub>CN molar emission ratios relative to CO of 0.11% for all vegetation types. These ratios are combined with a global biomass burning CO source estimate of  $700\text{ Tg CO yr}^{-1}$ . Biofuel source estimates are based on molar emission ratios relative to CO of 0.20% for HCN and 0.16% for CH<sub>3</sub>CN and a global biofuel CO source estimate of  $210\text{ Tg CO yr}^{-1}$ .

<sup>g</sup>Based on biomass burning and biofuel molar emission ratios relative to CO of 0.27% for HCN and 0.15% for CH<sub>3</sub>CN and a global biomass burning CO source estimate of  $700\text{ Tg CO yr}^{-1}$  [*Andreae and Merlet*, 2001]. Additional biogenic sources for both gases are invoked to balance estimated loss from ocean uptake.

<sup>h</sup>Global 3-D model study with biomass burning molar emission ratios relative to CO of 0.26% for HCN and 0.15% for CH<sub>3</sub>CN and a global biomass burning CO source estimate of  $487\text{ Tg CO yr}^{-1}$  [*Duncan et al.*, 2003]. The residential coal burning source (in Asia) is invoked to explain enhanced HCN and CH<sub>3</sub>CN in Chinese urban plumes. It assumes molar emission ratios relative to CO of 1.6% for HCN and 0.25% for CH<sub>3</sub>CN and a residential coal burning CO source in Asia of  $20\text{ Tg CO yr}^{-1}$ .

<sup>i</sup>Biomass burning source estimate is based on an emission ratio of  $2.6 \pm 1.7 \times 10^{-4}\text{ g CH}_3\text{CN g}^{-1}\text{ C}^{-1}$  for straw and savannah grass [*Lobert et al.*, 1991] and a global biomass burning carbon source estimate of  $3.1 \times 10^3\text{ Tg C yr}^{-1}$  [*Seiler and Crutzen*, 1980]. The automobile exhaust source estimate is based on a CH<sub>3</sub>CN emission factor of 1.3% g/g relative to organic compounds measured in the exhaust of a gasoline-powered engine [*Dulson*, 1978], combined with a global car exhaust source of organic compounds of  $21\text{ Tg yr}^{-1}$ .

<sup>j</sup>Based on biomass burning and biofuel CH<sub>3</sub>CN molar emission ratios (relative to CO) of 0.13% [*Holzinger et al.*, 1999] and a global biomass burning and biofuel CO source estimate of  $670\text{ Tg CO yr}^{-1}$ .

[8] Since the model simulations of HCN, CH<sub>3</sub>CN, and CO as implemented here are linear with respect to their sources, we resolve the contributions from different source regions and source types in the model by using tagged tracers [*Bey et al.*, 2001b], which can then be added to reconstitute the full concentration field. Tagged tracers resolve sources from biomass burning and residential coal burning, for Asia and for the rest of the world.

### 3. Model Sources and Sinks of HCN and CH<sub>3</sub>CN

#### 3.1. Sinks

##### 3.1.1. Ocean Uptake

[9] Constraints on ocean uptake for HCN and CH<sub>3</sub>CN can be obtained from the vertical gradients of concentrations

measured in background air over the North Pacific during TRACE-P [*Singh et al.*, 2003]. We implement this constraint here by using the observed gradients to infer a saturation ratio for these two gases that we can then extrapolate globally in the 3-D model simulation.

[10] Figure 1 shows the vertical distributions of HCN, CH<sub>3</sub>CN, and CO observed for the ensemble of the data in TRACE-P (dots and red lines). The CO mixing ratios decrease from the boundary layer to the free troposphere, while the opposite is seen in the mixing ratios of HCN and CH<sub>3</sub>CN. Median mixing ratios at 2–4 km are 220 pptv for HCN and 140 for CH<sub>3</sub>CN, while the corresponding values at 0–2 km are 195 and 104 pptv, respectively. This is consistent with an ocean sink for HCN and CH<sub>3</sub>CN and also with the dominant biomass burning source for these two

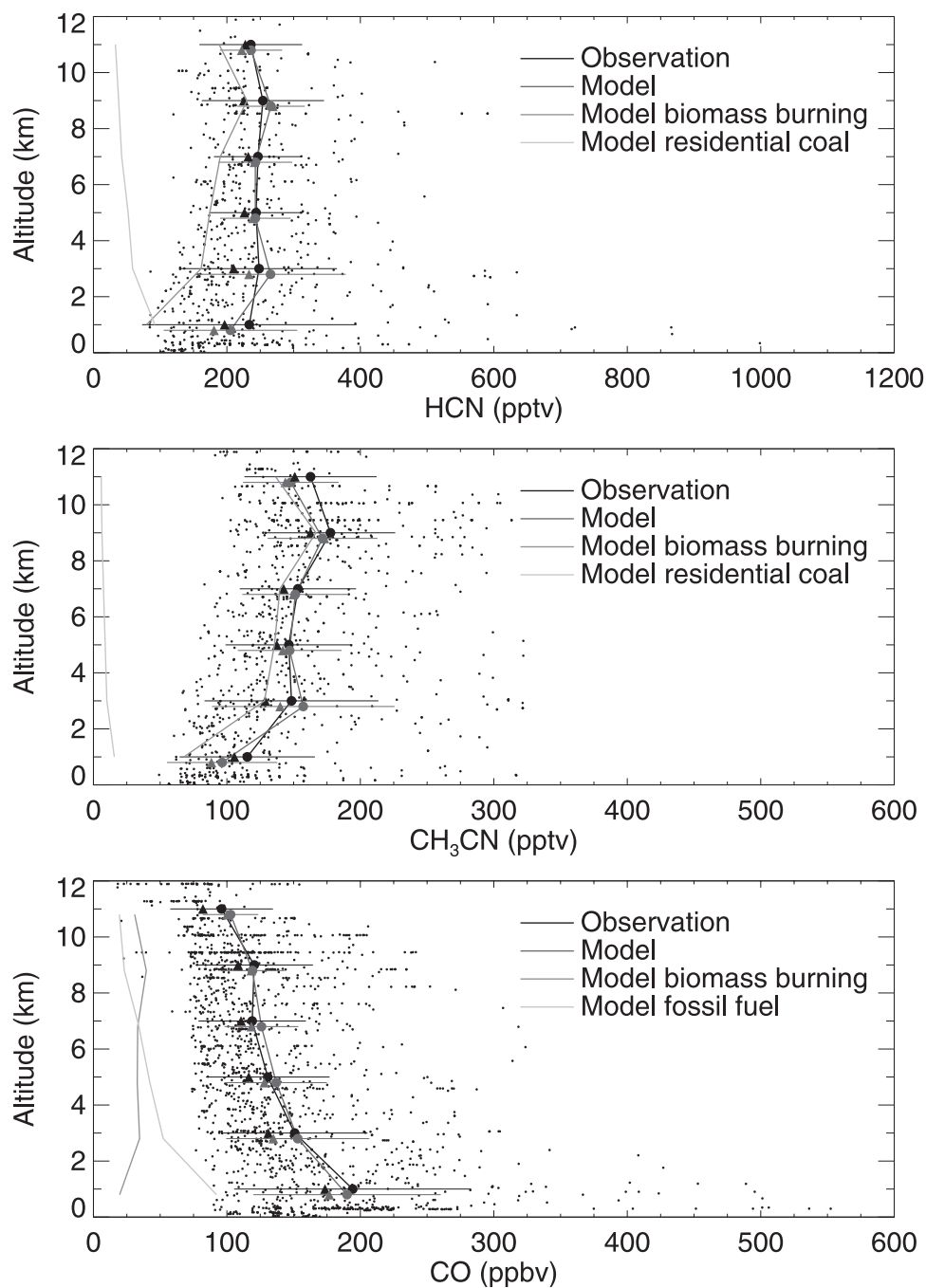


**Figure 1.** Vertical distributions of HCN, CH<sub>3</sub>CN, and CO for the ensemble of TRACE-P data over the NW Pacific (see *Jacob et al.* [2003] for a map of the area covered). Individual observations are shown as dots. Solid circles, triangles, and horizontal bars represent means, medians, and standard deviations, respectively. Model results are shown for the standard simulation and for tagged combustion tracers. Additional sources of CO in the model include biofuel burning and oxidation of methane and biogenic nonmethane hydrocarbons. See color version of this figure at back of this issue.

gases, in contrast to the large fossil fuel source for CO. Biomass burning outflow during TRACE-P was largely confined to the free troposphere, while there was considerable fossil fuel outflow in the boundary layer [*Carmichael et al.*, 2003; *Liu et al.*, 2003].

[11] Figure 2 shows the vertical distributions of HCN and CH<sub>3</sub>CN (dots and red lines) observed in TRACE-P

over the North Pacific under background conditions, defined here as CO < 120 ppbv and C<sub>2</sub>Cl<sub>4</sub> < 10 pptv [*Singh et al.*, 2003]. Both gases show significantly reduced mixing ratios in the marine boundary layer compared with their free tropospheric values. Asian outflow influence for these conditions is minimal, and the shape of the profiles is evidence for ocean uptake. Median

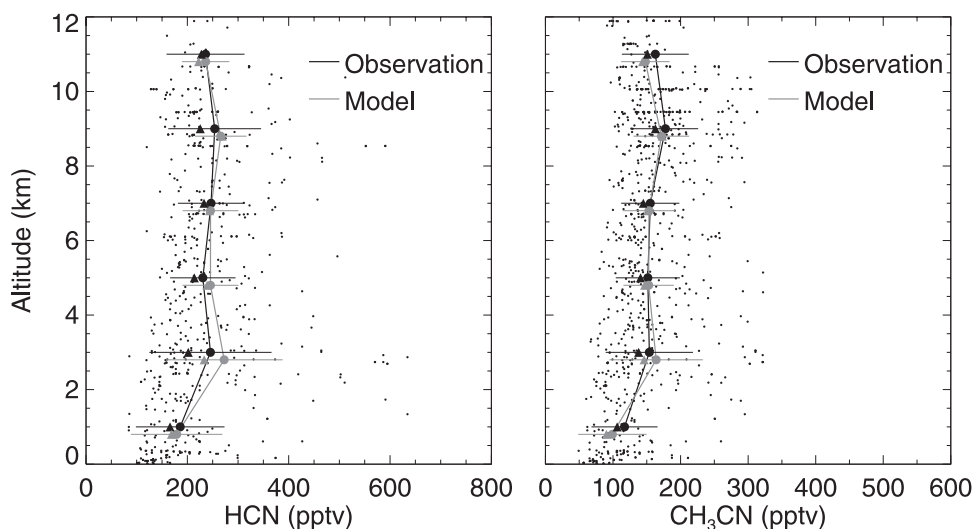


**Figure 2.** Vertical distributions of HCN and CH<sub>3</sub>CN observed in TRACE-P over the North Pacific under background conditions (CO < 120 ppbv and C<sub>2</sub>Cl<sub>4</sub> < 10 pptv). Individual observations are shown as dots. Solid circles, triangles, and horizontal bars represent means, medians, and standard deviations, respectively. See color version of this figure at back of this issue.

mixing ratios for these background conditions at 2–4 km are 201 pptv for HCN and 132 pptv for CH<sub>3</sub>CN, while the corresponding values at 0–2 km are 161 pptv and 106 pptv, respectively.

[12] Following *Singh et al.* [2003], the deposition velocities of HCN and CH<sub>3</sub>CN to the ocean can be derived using a box model of the marine boundary layer (MBL) with no divergence of horizontal flux [*Lenschow et al.*, 1983]. The resulting deposition velocity is 0.13 cm s<sup>-1</sup> for both gases. The comparable deposition velocities despite greater solubility of CH<sub>3</sub>CN imply faster consumption of HCN/CN<sup>-</sup> in the ocean (see discussion below). *de Laat et al.* [2001] previously inferred a deposition velocity of 0.01–0.05 cm s<sup>-1</sup> for CH<sub>3</sub>CN to the ocean in order to explain CH<sub>3</sub>CN mixing ratios observed in South Asian outflow to the Indian Ocean (INDOEX mission). *Warneke and de Gouw* [2001] estimated a deposition velocity of 0.34 cm s<sup>-1</sup> for CH<sub>3</sub>CN from ship measurements taken during an oceanic upwelling event. They attributed the higher value compared to that of *de Laat et al.* [2001] to the lower surface temperature and higher biological activity in the upwelling water. More recently, *de Gouw et al.* [2003] estimated a deposition velocity of 0.17 cm s<sup>-1</sup> for CH<sub>3</sub>CN from aircraft measurements over the NE Pacific.

[13] Using a two-layer film model for air-to-sea exchange [*Liss and Slater*, 1974], *Singh et al.* [2003] estimated saturation ratios of 0.77 for HCN and 0.83 for CH<sub>3</sub>CN from their TRACE-P data. We derive slightly different saturation ratios of 0.79 for HCN and 0.88 for CH<sub>3</sub>CN. The difference with *Singh et al.* [2003] reflects different assumptions on the parameterizations of conductances for mass transfer. In our 3-D model calculation we extrapolate these saturation ratios globally, resulting in atmospheric lifetimes against ocean uptake of 6 months for HCN and 8 months for CH<sub>3</sub>CN.

[14] Uptake of HCN and CH<sub>3</sub>CN by the ocean must require consumption (presumably biological) in the oceanic mixed layer OML, and we can readily estimate the implied

lifetimes. At steady state, the ocean uptake flux must be balanced by consumption in the OML

$$v_d C_{\text{MBL}} = \frac{Z}{\tau} C_{\text{OML}}, \quad (1)$$

$$S = H \frac{C_{\text{OML}}}{C_{\text{MBL}}}, \quad (2)$$

$$\tau = \frac{Z}{H} \frac{S}{v_d}, \quad (3)$$

where  $v_d$  is the deposition velocity,  $Z$  is the oceanic mixed layer depth (about 50 m for the middle-latitude North Pacific in March [*Kara et al.*, 2000]),  $\tau$  is the lifetime against consumption in the OML,  $C_{\text{MBL}}$  and  $C_{\text{OML}}$  are the respective concentrations in the MBL and OML,  $S$  is the saturation ratio, and  $H$  is the dimensionless Henry's law constant defined as the ratio of the concentration in air to that in seawater. Values for  $H$  at 298 K are  $3.4 \times 10^{-3}$  ( $\Delta H_{298}/R = 5000$  K) for HCN and  $7.6 \times 10^{-4}$  ( $\Delta H_{298}/R = 4100$  K) for CH<sub>3</sub>CN (*R. Sander, Henry's > law constants (solubilities), 2003, available at <http://www.mpch-mainz.mpg.de/~sander/res/henry.html>). The resulting lifetimes against consumption in the OML are three months for HCN(aq)/CN<sup>-</sup> and 14 months for CH<sub>3</sub>CN(aq)/CN<sup>-</sup>.*

### 3.1.2. Other Sinks

[15] Additional known losses for atmospheric HCN and CH<sub>3</sub>CN are reactions with OH and O(<sup>1</sup>D), photolysis, and precipitation scavenging. Of these, only reaction with OH is significant [*Cicerone and Zellner*, 1983; *Brasseur et al.*, 1983] and is implemented in the model using rate constants from *Wine et al.* [2002] for HCN and *DeMore et al.* [1997] for CH<sub>3</sub>CN, with monthly mean OH fields from a full chemistry simulation [*Li et al.*, 2002]. The recent laboratory study of *Wine et al.* [2002] indicates a factor of three lower rate constant for the HCN-OH reaction (low-pressure limit  $7.4 \times 10^{-33}$  cm<sup>6</sup> molecule<sup>-2</sup> s<sup>-1</sup>; high-pressure limit  $9.0 \times$

**Table 2.** Atmospheric Budgets of HCN and CH<sub>3</sub>CN

	HCN	CH <sub>3</sub> CN
Atmospheric burden, Tg N	0.426	0.28
Atmospheric lifetime, months	6.2	6.7
Tropospheric burden, <sup>a</sup> Tg N	0.38	0.25
Tropospheric lifetime, months	5.3	5.8
Sources, Tg N yr <sup>-1</sup>		
Biomass burning	0.63	0.47
Residential coal burning	0.2	0.03
Sinks, Tg N yr <sup>-1</sup>		
Ocean uptake	0.73	0.36
Reaction with OH	0.1	0.14

<sup>a</sup>For the 1000–100 hPa column.

$10^{-15}(T/300)^{3.2} \text{ cm}^3 \text{ molecule}^{-1} \text{ s}^{-1}$ , where  $T$  is temperature) than previously measured [Fritz *et al.*, 1984]. The corresponding lifetimes against oxidation by OH are 4.3 years for HCN and 2.2 years for CH<sub>3</sub>CN, much longer than the lifetimes against ocean uptake.

## 3.2. Sources

### 3.2.1. Biomass Burning

[16] Both HCN and CH<sub>3</sub>CN are mainly emitted in the low-temperature smoldering phase of biomass burning, similarly to CO [Lobert *et al.*, 1990]. Different fuel types and fire temperatures result in different emission ratios [Lobert *et al.*, 1991]. Past studies have indicated a large range of molar emission ratios for HCN (0.03–1.1%) and a narrower range for CH<sub>3</sub>CN (0.12–0.25%) [Lobert *et al.*, 1991; Hurst *et al.*, 1994a, 1994b; Yokelson *et al.*, 1997, 1999, 2003; Holzinger *et al.*, 1999; Goode *et al.*, 2000]. Emission ratios throughout this paper are in molar units relative to CO. When compounded with a range of global biomass burning CO emission estimates (200–800 Tg CO yr<sup>-1</sup>), one obtains global biomass burning sources of 0.1–3.2 m Tg N yr<sup>-1</sup> for HCN and 0.1–1.1 m Tg N yr<sup>-1</sup> for CH<sub>3</sub>CN (Table 1).

[17] The recent review of Andreae and Merlet [2001] recommends biomass burning HCN emission ratios of 0.05% (savanna and grassland) and 0.15% (tropical and extratropical forests) and a biomass burning CH<sub>3</sub>CN emission ratio of 0.11% for all vegetation types. The HCN recommendation for savanna and grassland is based on field experiments in Australia [Hurst *et al.*, 1994a, 1994b]. Recent measurements in African savanna fires show much higher HCN emission ratios ( $0.85 \pm 0.29\%$ ) [Yokelson *et al.*, 2003]. By averaging measurements of biomass burning emissions from different fuel types and from different regions of the world, Goode *et al.* [2000] found an average biomass burning HCN emission ratio of 0.34%, much higher than the Andreae and Merlet [2001] value.

[18] Correlations with CO in the TRACE-P observations provide important constraints on the emissions of HCN and CH<sub>3</sub>CN. Singh *et al.* [2003] used these correlations in biomass burning plumes to derive emission ratios of  $0.27 \pm 0.12\%$  for HCN and  $0.15 \pm 0.05\%$  for CH<sub>3</sub>CN. The HCN emission ratio is consistent with the average value reported by Goode *et al.* [2000], and is also in accord with the value of 0.28% estimated by Heald *et al.* [2003] based on multivariate analysis of the TRACE-P CO and HCN data. The CH<sub>3</sub>CN emission ratio is consistent with the Andreae and Merlet [2001] value. We find in GEOS-CHEM that the best fit to the TRACE-P observations of HCN, CH<sub>3</sub>CN, and

CO, and to the global HCN column data is obtained with biomass burning emission ratios of 0.27% for HCN and 0.20% for CH<sub>3</sub>CN, consistent with Singh *et al.* [2003]; we use these values in the simulations presented here. The corresponding sources of HCN and CH<sub>3</sub>CN in the model are 0.63 and 0.47 m Tg N yr<sup>-1</sup>, respectively (Table 2), within the range of past estimates (Table 1).

### 3.2.2. Residential Coal Burning Source in Asia

[19] It is well established that HCN and CH<sub>3</sub>CN are produced in the early stages of high-temperature combustion but are subsequently oxidized within the combustion chamber [Flagan and Seinfeld, 1988]. Direct measurements in automobile exhaust [Lobert *et al.*, 1991; Holzinger *et al.*, 2001] as well as aircraft measurements by Singh *et al.* [2003] and de Gouw *et al.* [2003] over southern California support that the source from fossil fuel combustion is negligible.

[20] However, TRACE-P observations show a strong enhancement of HCN, and a much weaker enhancement of CH<sub>3</sub>CN, in Chinese urban plumes sampled in the MBL less than two days downwind of the source [Singh *et al.*, 2003]. Figure 3 shows the HCN and CH<sub>3</sub>CN correlations with CO observed in three major Chinese urban plumes (DC-8 flights 9, 12, 13) sampled in the MBL during TRACE-P. Asian outflow in the MBL was in general advected behind cold fronts and was devoid of biomass burning influence [Carmichael *et al.*, 2003; Liu *et al.*, 2003]. The peak mixing ratios of HCN and CO observed in the Shanghai plume are 1.5 ppbv and 1 ppmv, respectively, while the peak mixing ratio for CH<sub>3</sub>CN is 300 pptv, much less enhanced. These peak mixing ratios were associated with high mixing ratios of CH<sub>3</sub>Cl [see Singh *et al.*, 2003, Figure 7a] and carbonyl sulfide (COS). The HCN-CO and CH<sub>3</sub>CN-CO correlations show slopes of 0.17% and 0.04%, respectively (Figure 3).

[21] Although there is widespread biofuel use in China [Streets *et al.*, 2003], data from Africa suggest negligible

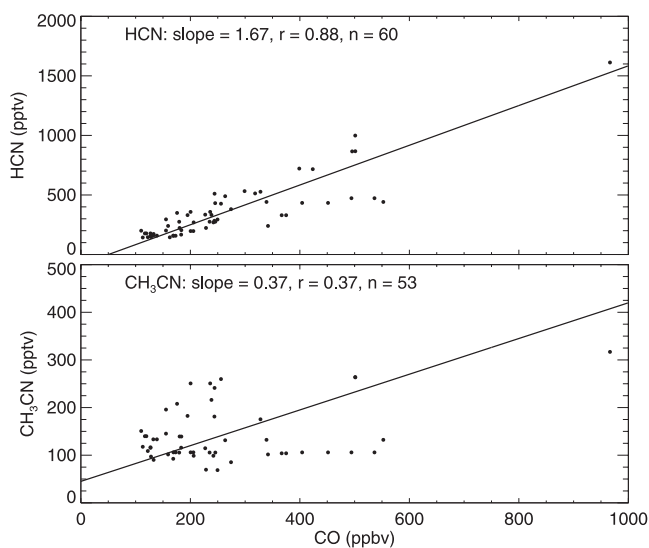


**Figure 3.** Observed (top) HCN and (bottom) CH<sub>3</sub>CN correlations with CO in three Chinese urban plumes sampled during TRACE-P (DC-8 flights 9, 12, and 13) below 2 km altitude. Regression lines (RMA method) are also shown.

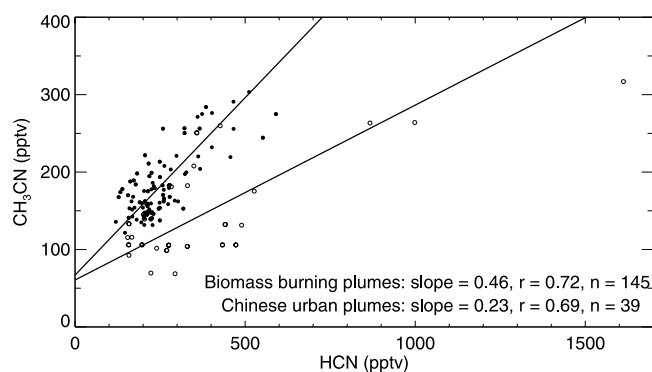


**Figure 4.** Observed CH<sub>3</sub>CN:HCN correlations in plumes sampled during TRACE-P. Solid circles are samples at 8–11 km on DC-8 flights 4, 7, 9, 12, 13, 14, 15, 17, 18, and 19; plumes at that altitude were largely devoid of anthropogenic influence [Liu *et al.*, 2003]. Open circles are Chinese urban plumes below 2 km (DC-8 flights 9, 12, and 13). Regression lines are shown.

nitrile emission from biofuels [Bertschi *et al.*, 2003; Yokelson *et al.*, 2003]. Also, the CH<sub>3</sub>CN/HCN enhancement ratio is much lower in the Chinese urban plumes than in biomass burning plumes (Figure 4). Singh *et al.* [2003] suggested that the enhancements of CH<sub>3</sub>Cl and COS correlated with enhanced HCN in the Chinese urban plumes could indicate a source from hard coal burning, and we follow that suggestion here. Clearly, further work is needed to identify the Chinese source of nitriles.

[22] We estimate the residential coal burning emission ratios of HCN and CH<sub>3</sub>CN relative to CO from the Chinese urban plumes observed in TRACE-P (Figure 3). Residential coal burning accounts for about 15% of anthropogenic CO emissions for China in the model. Combined with the slopes of the HCN-CO and CH<sub>3</sub>CN-CO correlations observed in the Chinese urban plumes (Figure 3), we obtain residential coal burning molar emission ratios of 1.2% for HCN and 0.26% for CH<sub>3</sub>CN relative to CO. Simulation of the TRACE-P data with GEOS-CHEM (section 4) indicates a best fit for residential coal burning emission ratios of 1.6% for HCN and 0.25% for CH<sub>3</sub>CN.

[23] When scaling the above emission ratios by the fraction of urban CO from residential coal burning in China, the resulting HCN/CO source ratio (0.24% for Shanghai, for example) is comparable to biomass burning (0.27%) while the resulting CH<sub>3</sub>CN/CO source ratio (0.04% for Shanghai, for example) is much lower than biomass burning (0.20%). The total residential coal burning sources in Asia in the model are 0.2 for HCN and 0.03 m Tg N yr<sup>-1</sup> for CH<sub>3</sub>CN (Table 2). This source could have a seasonal variation associated with heating [Streets *et al.*, 2003], but uncertainties are sufficiently large that we do not bother to include it here.

### 3.2.3. Biogenic Source

[24] There is indication that HCN is produced by higher plants [see Cicerone and Zellner, 1983, and references therein]. Recent laboratory results by Fall *et al.* [2001] show that wounded clover releases HCN in addition to large amounts of acetone. In the TRACE-P data, HCN is correlated with both acetone ( $r = 0.81$ , slope = 0.3 pptv ppbv<sup>-1</sup>,  $n = 746$ ) and methanol ( $r = 0.86$ , slope = 137 pptv ppbv<sup>-1</sup>,

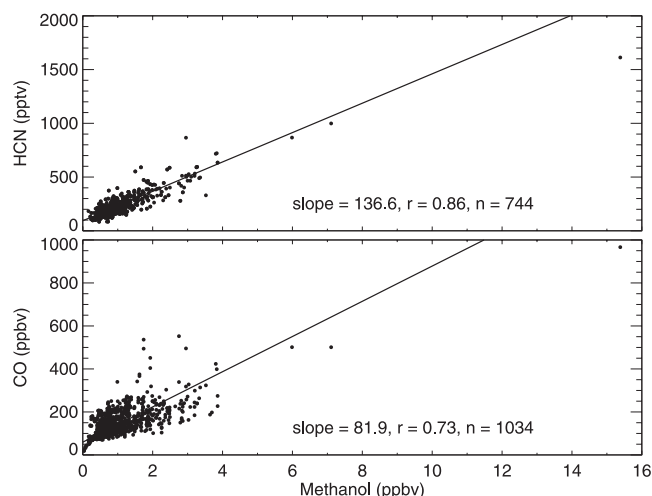


**Figure 5.** Observed HCN and CO correlations with methanol for the ensemble of TRACE-P data. Regression lines are shown.

$n = 744$ ), which have strong biogenic sources. In particular, methanol is generally considered a tracer for continental biogenic emissions [Heikes *et al.*, 2002]. Figure 5 (top) shows the correlation of HCN with methanol observed during TRACE-P. A similarly strong correlation was found for CH<sub>3</sub>CN. The biogenic source of methanol is estimated to be 50–280 Tg yr<sup>-1</sup> [Heikes *et al.*, 2002]. If the HCN-methanol correlation were to reflect a common biogenic source, then the implied biogenic HCN source would be

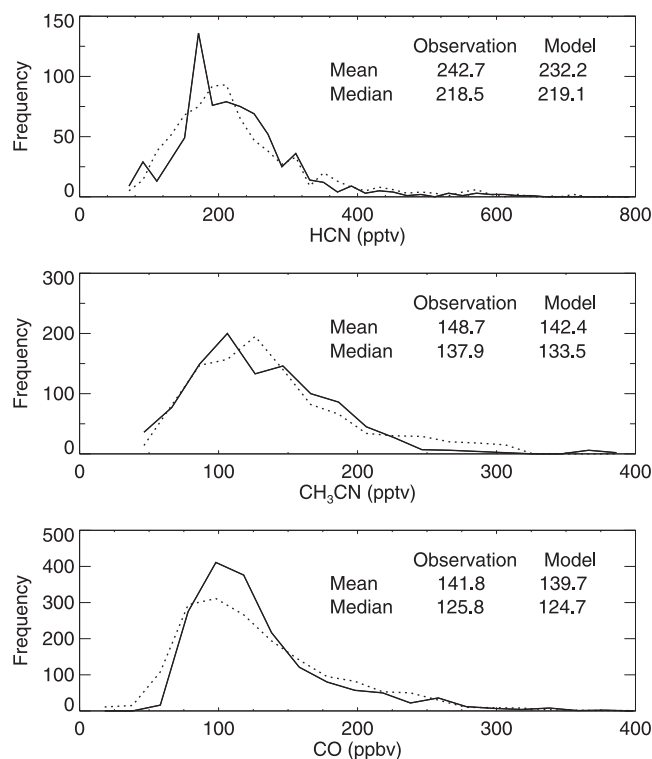


**Figure 6.** Frequency distributions of observed (solid line) and simulated (dashed line) mixing ratios of HCN, CH<sub>3</sub>CN, and CO for the ensemble TRACE-P data over the North Pacific.

3–17 m Tg N yr<sup>-1</sup>, far too large to be reconciled with the observed HCN concentrations [Li *et al.*, 2000]. Additionally, the highest methanol and HCN concentrations in TRACE-P were observed in the Chinese urban plumes. Methanol in TRACE-P was also strongly correlated with CO ( $r = 0.73$ , slope = 82 ppbv ppbv<sup>-1</sup>,  $n = 1034$ ) and was highest (together with HCN) in the Chinese urban plumes (Figure 5, bottom), implying an anthropogenic source. Thus we find no convincing evidence of a biogenic source of nitriles and do not include such a source in our simulations.

#### 4. Simulation of Observations

[25] In this section we examine the GEOS-CHEM model simulation of the TRACE-P observations for HCN and CH<sub>3</sub>CN and discuss what constraints this simulation provides. The model evaluation also considers CO, since our source specifications for HCN and CH<sub>3</sub>CN are based on relationships with CO. We also examine the consistency of our simulation with the global data sets of HCN columns previously used as constraints by Li *et al.* [2000] and with the INDOEX data of de Laat *et al.* [2001].

[26] As a general assessment of our simulation, in Figure 6 we show the frequency distributions of the observed and simulated HCN, CH<sub>3</sub>CN, and CO concentrations along the ensemble of TRACE-P flight tracks. The simulated mean and median values agree with the observed values to within 10 pptv for HCN, 5 pptv for CH<sub>3</sub>CN, and 5 ppbv for CO. There are no systematic biases or obvious anomalies in the simulated frequency distributions. Figure 7 shows scatterplots of simulated versus observed concentrations of HCN and CH<sub>3</sub>CN for the ensemble of TRACE-P data. The bulk of the points are strongly correlated, but the correlations are much smaller at high mixing ratios (primarily in the boundary layer), likely because of model errors in the location of plumes [Kiley *et al.*, 2003]. For further evaluation of the simulation we examine vertical distributions and correlations between species.

##### 4.1. Vertical Distributions

[27] The observed and simulated vertical profiles of HCN, CH<sub>3</sub>CN, and CO for the ensemble of TRACE-P measurements are shown in Figure 1. The model reproduces the increase of CO mixing ratios and the decrease of HCN and CH<sub>3</sub>CN mixing ratios from the free troposphere to the MBL. For the background conditions over the NW Pacific

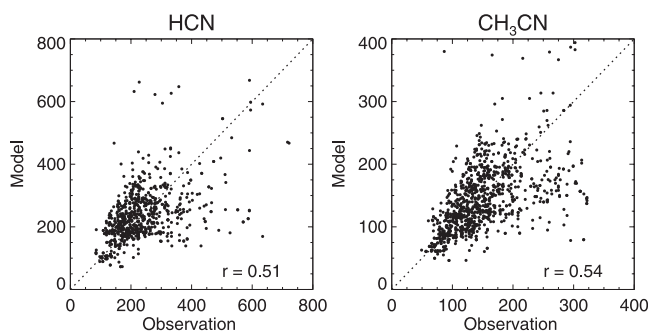


**Figure 7.** Scatterplots of simulated versus observed mixing ratios of HCN and CH<sub>3</sub>CN for the ensemble of TRACE-P data. The 1:1 line is also shown.

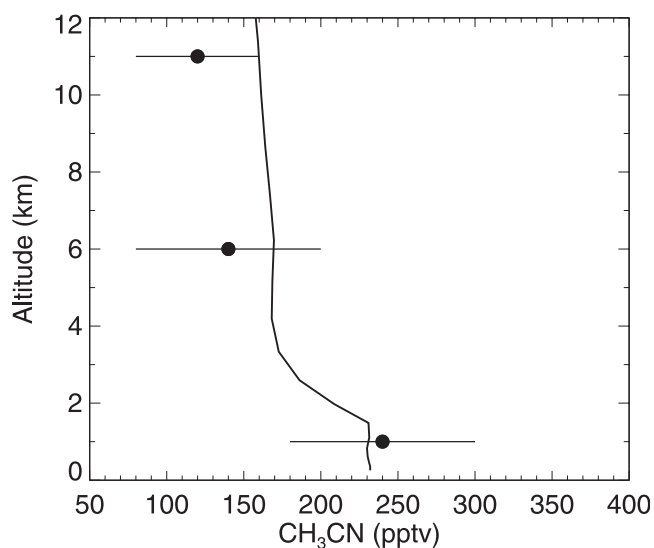


**Figure 8.** Vertical distribution of CH<sub>3</sub>CN concentrations over the northern Indian Ocean in March 2001. Median aircraft observations from the INDOEX campaign [de Laat *et al.*, 2001] are shown as symbols with standard deviations. Monthly mean model results for the corresponding month and region (0–10°N, 65°E–80°E) are shown as the solid line.

(Figure 2), the model reproduces the gradients of HCN and CH<sub>3</sub>CN between the free troposphere and the MBL driven by ocean uptake. Without ocean uptake in the model there would be no such gradients. Also shown in Figure 1 are the relative contributions from biomass burning and residential coal burning simulated in the model using tagged tracers. Biomass burning accounts for 70–85% of total HCN and 90–95% of total CH<sub>3</sub>CN in the free troposphere (above 2 km), while in the boundary layer the fractions are 45% and 75%, respectively. Thus it appears that CH<sub>3</sub>CN is a better tracer for biomass burning. Simulated and observed mean vertical profiles of HCN and CH<sub>3</sub>CN show enhancements at 2–4 km and 8–11 km (Figure 1). These correspond to preferential altitudes for frontal and convective outflow of biomass burning pollution, respectively [Bey *et al.*, 2001b; Liu *et al.*, 2003].

[28] We also compare model results in Figure 8 to aircraft measurements of CH<sub>3</sub>CN made over the northern Indian Ocean during the INDOEX campaign [de Laat *et al.*, 2001]. In contrast to TRACE-P, the INDOEX observations show maximum concentrations in the MBL due to boundary layer outflow from the Indian subcontinent associated with the winter-spring monsoon. The model reproduces this enhancement, which is thus consistent with our representation of the ocean sink.

##### 4.2. Correlations Between HCN, CH<sub>3</sub>CN, and CO

[29] Figure 9 compares the observed and simulated correlations between HCN, CH<sub>3</sub>CN, and CO for the ensemble of the TRACE-P data in the free troposphere and in the boundary layer. The model reproduces the slopes of the correlations to within their expected errors. Differences in slopes between the free troposphere and the boundary layer reflect the dominant influence of biomass burning in the free troposphere, and the added influences from the urban source

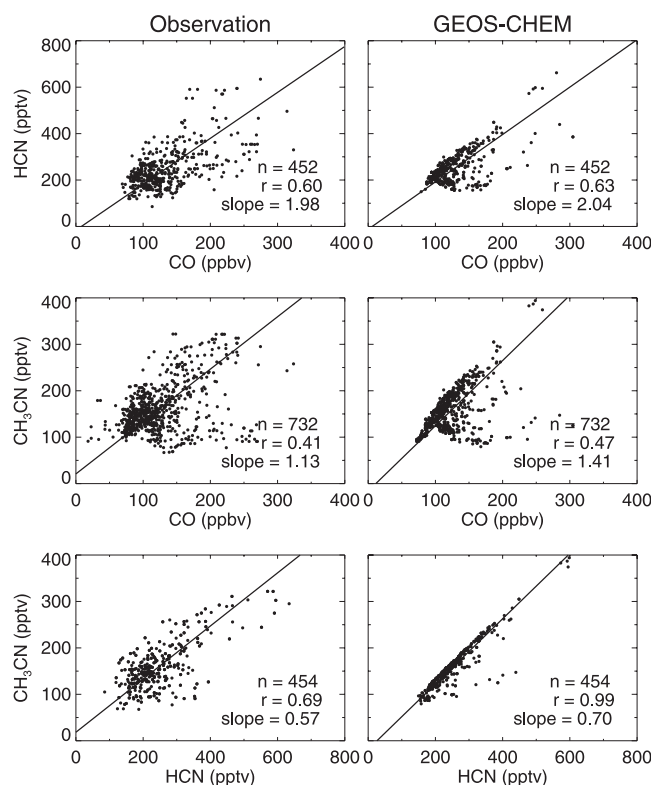


**Figure 9a.** Observed and simulated HCN-CH<sub>3</sub>CN-CO correlations in the free troposphere (above 2 km) during TRACE-P. Regression lines and correlation coefficients are shown.

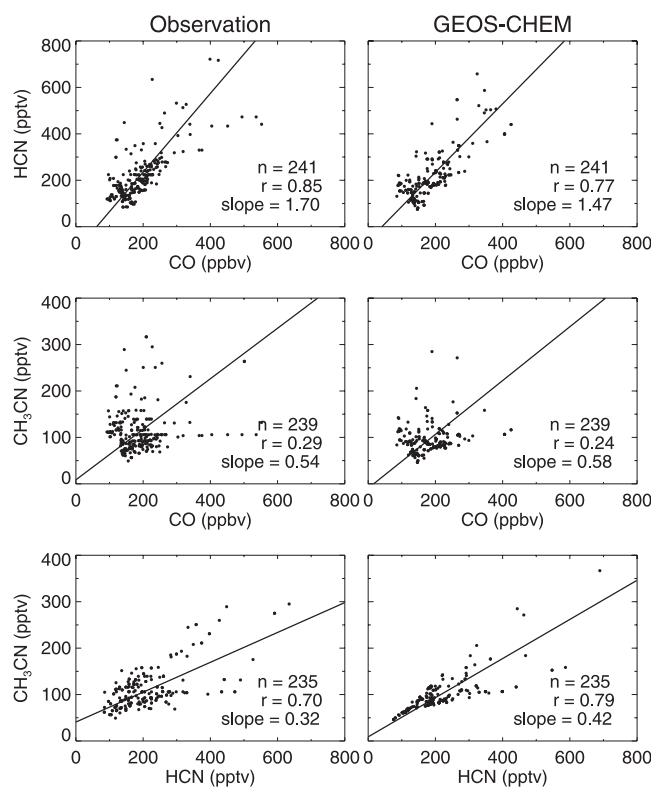


**Figure 9b.** Same as Figure 9a but for the boundary layer (below 2 km).

and the deposition sink in the MBL. The CH<sub>3</sub>CN-CO correlation is poor in the boundary layer ( $r = 0.29$  in the observations and  $r = 0.24$  in the model), while the HCN-CO correlation is strong ( $r = 0.85$  in the observations and  $r = 0.77$  in the model), reflecting the similarity between urban and biomass burning emission ratios for HCN/CO but the much lower urban ratios for CH<sub>3</sub>CN/CO. The CH<sub>3</sub>CN-HCN correlation in the free troposphere above 2 km (Figure 9a) shows less variability in the model than in the observations, which likely reflects the assumption of uniform biomass burning emission ratios of HCN and CH<sub>3</sub>CN in the model, while in reality these emission ratios vary for different fuel types and fire temperatures [Lobert *et al.*, 1991]. The CH<sub>3</sub>CN-CO relationship in the boundary layer (Figure 9b) shows two branches, both in the model and in the observations, reflecting (1) the subsidence of biomass burning influence from the free troposphere (high CH<sub>3</sub>CN, low CO) and (2) the urban outflow influence (low CH<sub>3</sub>CN, high CO).

### 4.3. HCN Columns

[30] Spectroscopic measurements of HCN atmospheric columns were made at three Japanese sites during TRACE-P as part of a long-term observational program [Zhao *et al.*, 2000, 2002]. The three sites are Moshiri (44° N, 142° E, 0.28 km altitude), Rikubetsu (43.5° N, 144° E, 0.37 km altitude), and Tsukuba (36° N, 140° E, 0.03 km altitude). The data for the TRACE-P period are shown in Figure 10 (solid circles). The columns at Tsukuba show much higher variation than at Moshiri and Rikubetsu, reflecting the latitudinal difference and the proximity of Tsukuba to the main channel of Asian outflow at 25°N–

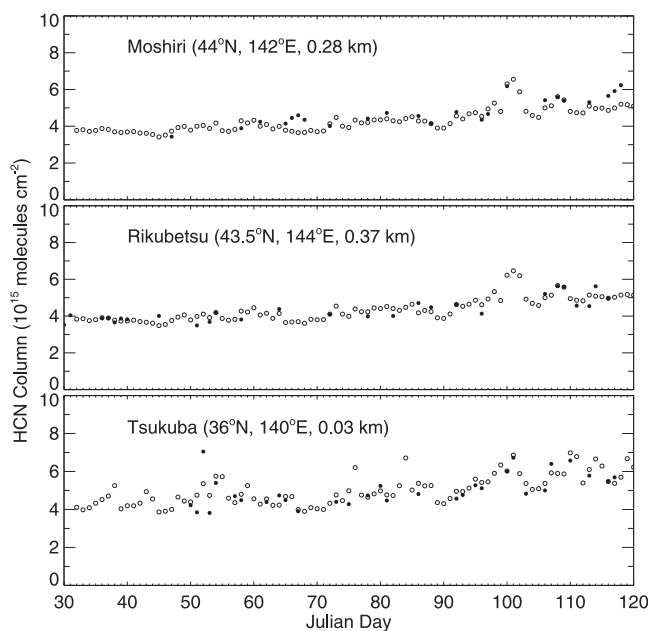


**Figure 10.** Time series of observed (solid circles) and simulated (open circles) 24-hour average HCN columns ( $\text{molecules cm}^{-2}$ ) at the three Japanese stations of Moshiri (44°N, 142°E, 0.28 km altitude), Rikubetsu (43.5°N, 144°E, 0.37 km altitude), and Tsukuba (36°N, 140°E, 0.03 km altitude) during TRACE-P (February–April 2001).

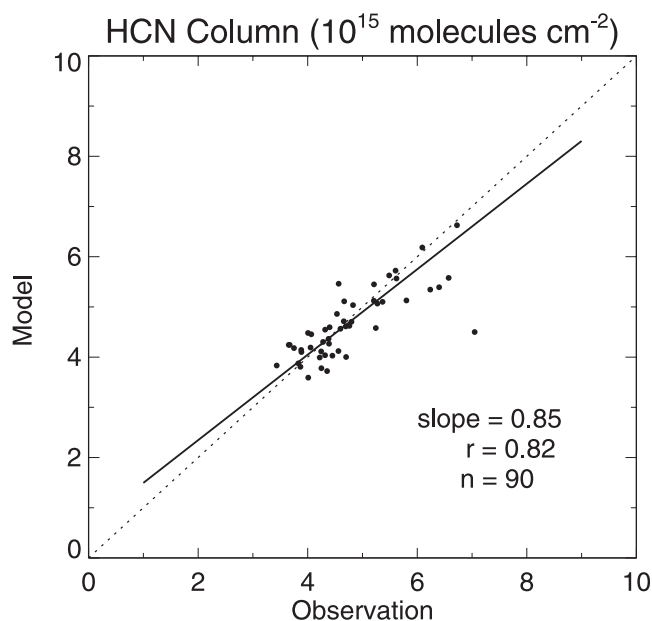


**Figure 11.** Scatterplot of observed and simulated daily HCN columns (molecules cm<sup>-2</sup>) at the Moshiri, Rikubetsu, and Tsukuba Japanese sites during TRACE-P. Values are averages over the three sites. The regression line is calculated without the outlier.

35°N [Bey *et al.*, 2001b; Liu *et al.*, 2003]. The increases in the columns from February to April are consistent with the previous observation of a spring-summer HCN column maximum at these sites [Zhao *et al.*, 2000, 2002], and can be explained by the seasonal variation of biomass burning emissions [Li *et al.*, 2000].

[31] Figure 10 compares model results for the TRACE-P period with observed HCN columns at the three Japanese sites. The averaging kernel and a priori vertical profile from the retrievals [Zhao *et al.*, 2000, 2002] were applied to the model results. The HCN columns average  $4 \times 10^{15}$  molecules cm<sup>-2</sup> with high values of  $5-7 \times 10^{15}$  molecules cm<sup>-2</sup>, both in the observations and the model, consistent with previous column measurements at northern middle latitudes [Mahieu *et al.*, 1995, 1997; Zhao *et al.*, 2000, 2002]. A scatterplot of simulated versus observed HCN columns is shown in Figure 11. There is strong correlation ( $r = 0.82$ ), reflecting in part the seasonal increase from February to April (Figure 12), and no significant bias.

[32] Multiyear measurements of HCN columns are available from several sites in the Northern Hemisphere and provide another important test for the model. We used these data of Li *et al.* [2000] to evaluate our previous simulation of HCN. The present model has a weaker HCN source and a longer HCN lifetime to match the TRACE-P constraints, and it is imperative to determine whether these changes degrade the simulation of the HCN column data. Figure 12 compares model results for 2000 to the seasonal variations in these multiyear records, including data from the Japanese sites [Zhao *et al.*, 2000, 2002], Kitt Peak in Arizona [Mahieu *et*

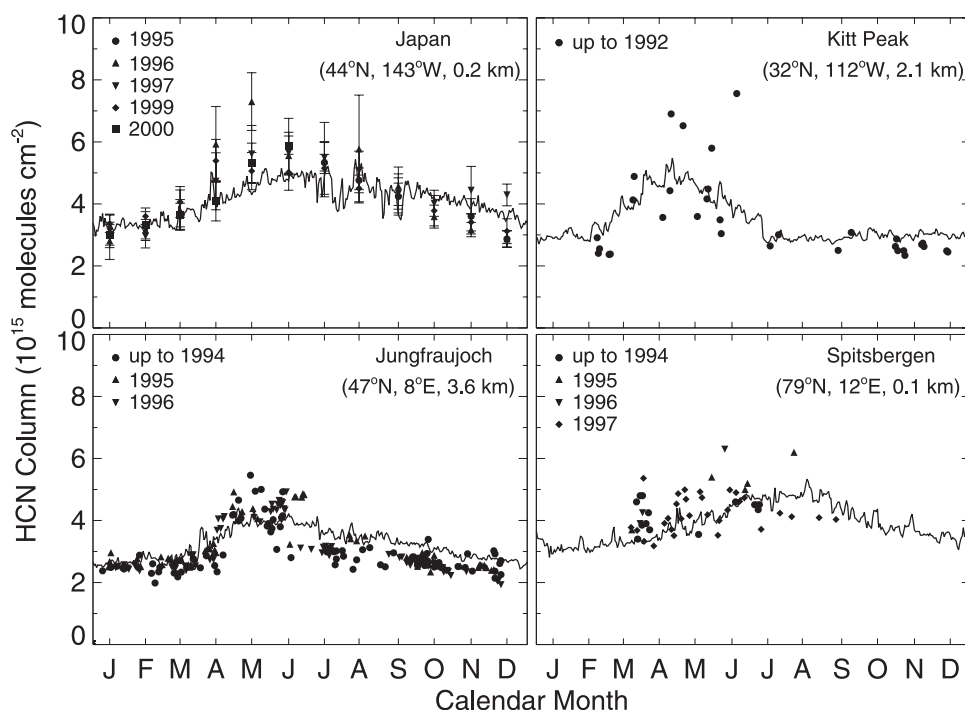


**Figure 12.** Monthly mean HCN total columns (molecules cm<sup>-2</sup>) retrieved from spectroscopic measurements at Moshiri and Rikubetsu in Japan [Zhao *et al.*, 2000, 2002], Kitt Peak in Arizona [Mahieu *et al.*, 1995], Jungfrauoch in the Swiss Alps [Mahieu *et al.*, 1995, 1997], and Ny Ålesund in Spitsbergen [Li *et al.*, 2000]. Data for the two Japanese sites are monthly means and vertical bars indicate standard deviations. The solid lines represent simulated daily average HCN total columns for 2000.

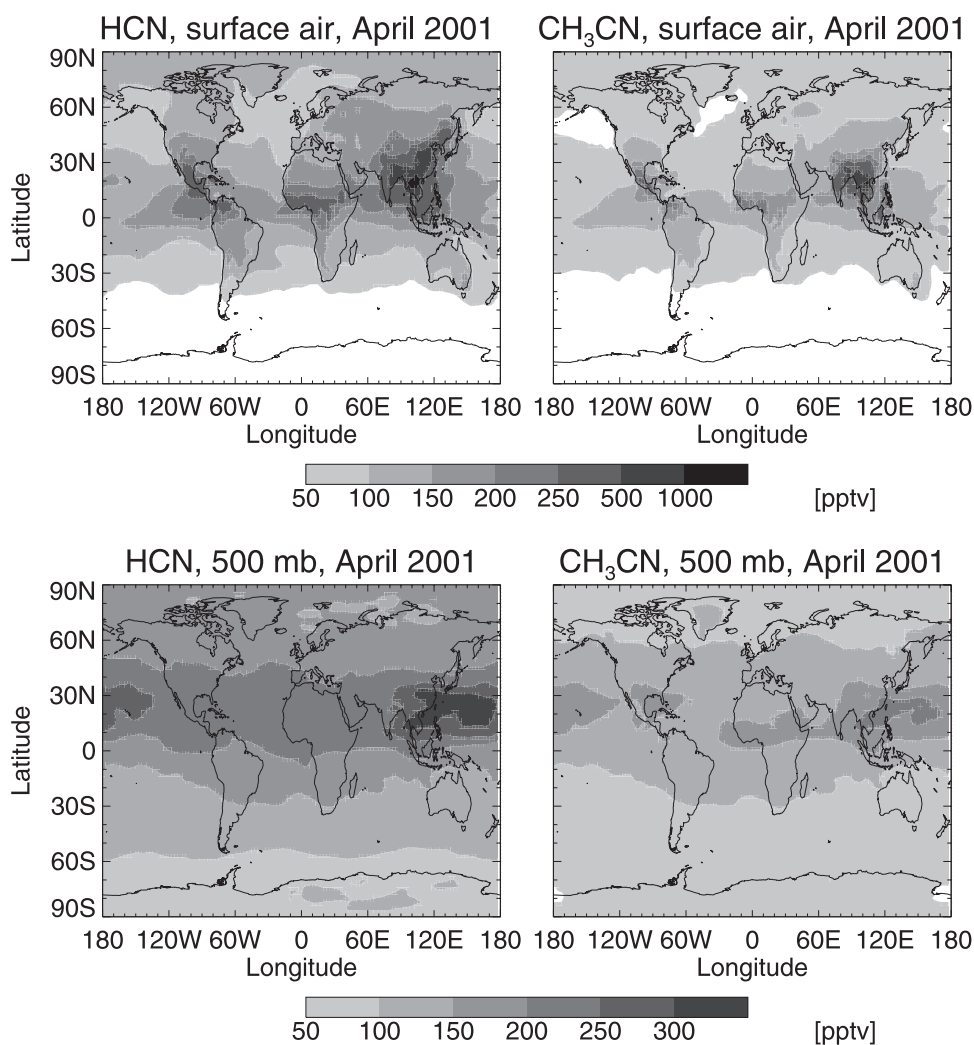


**Figure 13.** Simulated global distributions of HCN and CH<sub>3</sub>CN concentrations in surface air and at 500 hPa for April 2001. See color version of this figure at back of this issue.

*al.*, 1995], Jungfraujoch in the Swiss Alps [Mahieu *et al.*, 1995, 1997], and Ny Ålesund in Spitsbergen [Li *et al.*, 2000]. Observations for 1998 were excluded because of anomalous fire influence throughout the Northern Hemisphere [Rinsland *et al.*, 1999, 2000; Zhao *et al.*, 2002]. We find that we achieve a similar or better simulation than in the study of Li *et al.* [2000]. The reader is referred to that paper for discussion of the seasonal features.

## 5. Global Budgets and Distributions of HCN and CH<sub>3</sub>CN

[33] The global atmospheric budgets of HCN and CH<sub>3</sub>CN in the model are shown in Table 2. Biomass burning contributes 0.63 m Tg N yr<sup>-1</sup> to global HCN and 0.47 m Tg N yr<sup>-1</sup> to global CH<sub>3</sub>CN, while the corresponding sources from residential coal burning in Asia are 0.2 and 0.03 m Tg N yr<sup>-1</sup>, respectively. Ocean uptake dominates the loss of both HCN (0.73 m Tg N yr<sup>-1</sup>) and CH<sub>3</sub>CN (0.36 m Tg N yr<sup>-1</sup>), while the sink from reaction with OH is relatively small (0.1 m Tg N yr<sup>-1</sup> for HCN and 0.13 m Tg N yr<sup>-1</sup> for CH<sub>3</sub>CN). The resulting tropospheric lifetimes

(for the 1000–100 hPa column) are 5.3 months for HCN and 5.8 months for CH<sub>3</sub>CN.

[34] Our HCN lifetime is longer, and the implied global source smaller, than in our previous study [Li *et al.*, 2000] using the constraints from the observed relative seasonal variation of HCN columns [Li *et al.*, 2000, Table 1]. In that study we used the relative seasonal amplitude of the observed columns as constraint on the HCN lifetime and derived a global source by mass balance. We considered that the seasonal amplitude of the columns constrained the lifetime to be less than 4 months, where as the TRACE-P constraints imply a longer lifetime (5.3 months). As shown in Figure 12, it appears that this longer lifetime is still compatible with the constraints from the HCN column observations.

[35] Figure 13 shows simulated global mean distributions of HCN and CH<sub>3</sub>CN in April 2001. Surface concentrations are maximum over biomass burning regions in SE Asia, central America, and central Africa (>1000 pptv). Surface concentrations are very low (<50 pptv) at high southern latitudes, reflecting the remoteness from sources and the sink from ocean uptake under our assumption of uniform

saturation ratios. Observations in this part of the world are evidently needed. Concentrations in the middle troposphere at 500 hPa are highest over SE Asia and downwind, with a circumpolar band of relatively high concentrations (>200 pptv for HCN) at 5°N–40°N due to biomass burning influence.

## 6. Conclusions

[36] We used a global 3-D model analysis of in situ HCN-CH<sub>3</sub>CN-CO aircraft observations made over the NW Pacific during the TRACE-P aircraft mission (February–April 2001) to improve understanding of the atmospheric budgets of both gases. Vertical gradients of HCN and CH<sub>3</sub>CN observed in remote marine air confirm the previous hypotheses of a dominant ocean sink for HCN [Li *et al.*, 2000] and CH<sub>3</sub>CN [Hamm and Warneck, 1990]. Following Singh *et al.* [2003], we used these gradients to derive deposition velocities of 0.13 cm s<sup>-1</sup> for both gases, corresponding to saturation ratios of 0.79 for HCN and 0.88 for CH<sub>3</sub>CN. These deposition velocities imply lifetimes of three months for HCN(aq)/CN<sup>-</sup> and 14 months for CH<sub>3</sub>CN(aq)/CN<sup>-</sup> against consumption in the oceanic mixed layer.

[37] Biomass burning plumes from SE Asia observed during TRACE-P confirmed the importance of biomass burning as a global source for HCN and CH<sub>3</sub>CN, while observations in southern California confirmed that automobile exhaust is not a significant source for either gas [Singh *et al.*, 2003]. However, HCN and CH<sub>3</sub>CN observed in fresh Chinese urban plumes indicate emissions of anthropogenic origin with a much higher HCN/CH<sub>3</sub>CN ratio than from biomass burning. We tentatively attribute these enhancements to residential coal burning in Asia.

[38] Our global model uses biomass burning and residential coal burning emission ratios (molar) relative to CO of 0.27% and 1.6% respectively for HCN, and 0.2% and 0.25%, respectively, for CH<sub>3</sub>CN, as providing the best fit to the TRACE-P observations within the constraints offered by the HCN-CH<sub>3</sub>CN-CO relationships observed in biomass burning and urban plumes. The resulting simulation captures the observed frequency distributions of HCN and CH<sub>3</sub>CN concentrations in TRACE-P, their vertical distributions, and their correlations with CO. It offers a good simulation of ground-based measurements of HCN columns, at sites in Japan and elsewhere in the Northern Hemisphere, both during TRACE-P and over the multiyear record. It also reproduces the mean CH<sub>3</sub>CN vertical distribution observed over the northern Indian Ocean during the INDOEX aircraft campaign.

[39] Our global budgets of HCN and CH<sub>3</sub>CN indicate biomass burning sources of 0.63 and 0.47 m Tg N yr<sup>-1</sup>, respectively, and residential coal burning sources in Asia of 0.2 and 0.03 m Tg N yr<sup>-1</sup>, respectively. Ocean uptake is the dominant sink for both; oxidation by OH is an additional minor sink. The resulting tropospheric lifetimes are 5.3 months for HCN and 5.8 months for CH<sub>3</sub>CN. The HCN lifetime is longer, and the global source smaller, than in our previous model analysis [Li *et al.*, 2000], but it still provides an unbiased simulation of the relative seasonal cycle of HCN columns which was the main constraint in that previous analysis. The model predicts maximum surface air concentrations of HCN and CH<sub>3</sub>CN over biomass

burning regions and very low (<50 pptv) concentrations at high southern latitudes due to ocean uptake under the assumption of a uniform saturation ratio. Observations are evidently needed to test this assumption. Concentrations in the middle troposphere are highest over tropical biomass burning regions and downwind, with a circumpolar band of high concentrations at 5°N–40°N. Although both HCN and CH<sub>3</sub>CN appear to be good tracers of biomass burning in the free troposphere, CH<sub>3</sub>CN is a better tracer in the boundary layer due to the relatively large Chinese urban source of HCN. More work is needed to characterize the nature of this Chinese urban source.

[40] **Acknowledgments.** Discussions with Jennifer Logan and Rose Yevich were very helpful. This work was funded by the Atmospheric Chemistry Program of the U.S. National Science Foundation and by the NASA Global Tropospheric Chemistry Program.

## References

- Andreae, M. O., and P. Merlet, Emission of trace gases and aerosols from biomass burning, *Global Biogeochem. Cycles*, **15**, 955–966, 2001.
- Bange, H. W., and J. Williams, New directions: Acetonitrile in atmospheric and biogeochemical cycles, *Atmos. Environ.*, **34**, 4959–4960, 2000.
- Bertschi, I., et al., The trace gas and particle emissions from fires in large-diameter and belowground biomass fuels, *J. Geophys. Res.*, **108**(D13), 8472, doi:10.1029/2002JD002100, 2003.
- Bey, I., et al., Global modeling of tropospheric chemistry with assimilated meteorology: Model description and evaluation, *J. Geophys. Res.*, **106**, 23,073–23,095, 2001a.
- Bey, I., D. J. Jacob, J. A. Logan, and R. M. Yantosca, Asian chemical outflow to the Pacific: Origins, pathways and budgets, *J. Geophys. Res.*, **106**, 23,097–23,113, 2001b.
- Blake, N., et al., Large-scale latitudinal and vertical distributions of NMHCs and selected halocarbons in the troposphere over the Pacific Ocean during the March–April 1999 Pacific Exploratory Mission (PEM-Tropics B), *J. Geophys. Res.*, **106**, 32,627–32,644, 2001.
- Brasseur, G., E. Arijs, A. de Rudder, D. Nevejans, and J. Ingels, Acetonitrile in the atmosphere, *Geophys. Res. Lett.*, **10**, 725–728, 1983.
- Carmichael, G. R., et al., Regional-scale chemical transport modeling in support of intensive field experiments: Overview and analysis of the TRACE-P observations, *J. Geophys. Res.*, **108**(D21), 8823, doi:10.1029/2002JD003117, in press, 2003.
- Chan, L. Y., C. Y. Chan, H. Y. Liu, S. A. Christopher, S. J. Oltmans, and J. M. Harris, A case study on the biomass burning in southeast Asia and enhancement of tropospheric ozone over Hong Kong, *J. Geophys. Res.*, **27**, 1479–1482, 2000.
- Cicerone, R. J., and R. Zellner, The atmospheric chemistry of hydrogen cyanide (HCN), *J. Geophys. Res.*, **88**, 10,689–10,696, 1983.
- Crutzen, P. J., and M. O. Andreae, Biomass burning in the tropics: Impact on atmospheric chemistry and biogeochemical cycles, *Science*, **250**, 1669–1678, 1990.
- de Fré, R., P. Bruynseraede, and J. Kretzschmar, Air pollution measurements in traffic tunnels, *Environ. Health Perspect.*, **102**, 31–37, 1994.
- de Gouw, J. A., C. Warneke, D. D. Parrish, J. S. Holloway, M. Trainer, and F. C. Fehsenfeld, Emission sources and ocean uptake of acetonitrile (CH<sub>3</sub>CN) in the atmosphere, *J. Geophys. Res.*, **108**(D11), 4329, doi:10.1029/2002JD002897, 2003.
- de Laat, A. T. J., J. A. de Gouw, J. Lelieveld, and A. Hansel, Model analysis of trace gas measurements and pollution impact during INDOEX, *J. Geophys. Res.*, **106**, 28,469–28,480, 2001.
- DeMore, W. B., et al., Chemical kinetics and photochemical data for use in stratospheric modeling, *JPL Publ.*, **97-4**, 1997.
- Dulson, W., *Organisch-chemische Fremdstoffe in atmosphärischer Luft*, *Schr. Ver. Wasser Boden Lufthygiene*, **47**, Gustav Fischer, Stuttgart, Germany, 1978.
- Duncan, B. N., J. A. Logan, A. C. Staudt, R. Yevich, and J. A. Logan, Interannual and seasonal variability of biomass burning emissions constrained by satellite observations, *J. Geophys. Res.*, **108**(D2), 4100, doi:10.1029/2002JD002378, 2003.
- Fall, R., S. Kato, and V. M. Bierbaum, New directions: The biogenic acetone-HCN connection, *Atmos. Environ.*, **35**, 1713–1714, 2001.
- Flagan, R. C., and J. H. Seinfeld, *Fundamentals of Air Pollution Engineering*, Chapter 3, Prentice-Hall, Englewood Cliffs, N. J., 1988.
- Fritz, B., K. Lorenz, W. Steinert, and R. Zellner, Rate of oxidation of HCN by OH radicals at lower temperatures, *Oxid. Commun.*, **6**, 363–370, 1984.

- Goode, J. G., et al., Measurements of excess O<sub>3</sub>, CO<sub>2</sub>, CO, CH<sub>4</sub>, C<sub>2</sub>H<sub>4</sub>, C<sub>2</sub>H<sub>2</sub>, HCN, NO, NH<sub>3</sub>, HCOOH, CH<sub>3</sub>COOH, HCHO, and CH<sub>3</sub>OH in 1997 Alaskan biomass burning plumes by Airborne Fourier Transform Infrared Spectroscopy (AFTIR), *J. Geophys. Res.*, *105*, 22,147–22,166, 2000.
- Hamm, S., and P. Warneck, The interhemispheric distribution and the budget of acetonitrile in the troposphere, *J. Geophys. Res.*, *95*, 20,593–20,606, 1990.
- Heald, C., D. J. Jacob, P. I. Palmer, M. J. Evans, G. W. Sachse, H. Singh, and D. Blake, Biomass burning emission inventory with daily resolution: Application to aircraft observations of Asian outflow, *J. Geophys. Res.*, *108*(D21), 8811, doi:10.1029/2002JD003082, in press, 2003.
- Heikes, B., et al., Ozone, hydroperoxides, oxides of nitrogen, and hydrocarbon budgets in the marine boundary layer over the South Atlantic, *J. Geophys. Res.*, *101*, 24,221–24,234, 1996.
- Heikes, B., et al., Atmospheric methanol budget and ocean implication, *Global Biogeochem. Cycles*, *16*(D4), 1133, doi:10.1029/2002GB001895, 2002.
- Holzinger, R., et al., Biomass burning as a source of formaldehyde, acetaldehyde, methanol, acetone, acetonitrile, and hydrogen cyanide, *J. Geophys. Res.*, *26*, 1161–1164, 1999.
- Holzinger, R., A. Jordan, A. Hansel, and W. Lindinger, Automobile emissions of acetonitrile: Assessments of its contribution to the global source, *Atmos. Environ.*, *38*, 187–193, 2001.
- Hurst, D. F., D. W. T. Griffith, and G. D. Cook, Trace gas emissions from biomass burning in tropical Australian savannas, *J. Geophys. Res.*, *99*, 16,441–16,456, 1994a.
- Hurst, D. F., D. W. T. Griffith, J. N. Carras, D. J. Williams, and P. J. Fraser, Measurements of trace gases emitted by Australian savanna fires during the 1990 dry season, *J. Atmos. Chem.*, *18*, 33–56, 1994b.
- Jacob, D. J., J. Crawford, M. M. Kleb, V. S. Connors, R. J. Bendura, J. L. Raper, G. W. Sachse, J. Gille, L. Emmons, and J. C. Heald, Transport and Chemical Evolution over the Pacific (TRACE-P) mission: Design, execution, and first results, *J. Geophys. Res.*, *108*(D20), 9000, doi:10.1029/2002JD003276, 2003.
- Kara, A. B., P. A. Rochford, and H. E. Hurlburt, Mixed layer depth variability and barrier layer formation over the North Pacific Ocean, *J. Geophys. Res.*, *105*, 16,783–16,801, 2000.
- Kiley, C., et al., An intercomparison and evaluation of aircraft-derived and simulated CO from seven chemical transport models during the TRACE-P experiment, *J. Geophys. Res.*, *108*(D21), 8819, doi:10.1029/2002JD003089, in press, 2003.
- Lenschow, D. H., R. Pearson Jr., and B. B. Stankov, Measurements of ozone vertical flux to ocean and forest, *J. Geophys. Res.*, *87*, 8833–8837, 1983.
- Li, Q., D. J. Jacob, I. Bey, R. M. Yantosca, Y. Zhao, Y. Kondo, and J. Notholt, Atmospheric hydrogen cyanide (HCN): Biomass burning source, ocean sink?, *Geophys. Res. Lett.*, *27*, 357–360, 2000.
- Li, Q., et al., Transatlantic transport of pollution and its effects on surface ozone in Europe and North America, *J. Geophys. Res.*, *107*(D13), doi:10.1029/2001JD001422, 2002.
- Liss, P. S., and P. G. Slater, Flux of gases across the air-sea interface, *Nature*, *247*, 181–184, 1974.
- Liu, H., W. L. Chang, S. J. Oltmans, L. Y. Chan, and J. M. Harris, On springtime high ozone events in the lower troposphere from southeast Asian biomass burning, *Atmos. Environ.*, *33*, 2403–2410, 1999.
- Liu, H., D. J. Jacob, I. Bey, R. Yantosca, B. N. Duncan, and G. W. Sachse, Transport pathways for Asian pollution outflow over the Pacific: Interannual and seasonal variations, *J. Geophys. Res.*, *108*(D20), 8786, doi:10.1029/2002JD003102, 2003.
- Lober, J. M., D. H. Scharffe, W. M. Hao, and P. J. Crutzen, Importance of biomass burning in the atmospheric budgets of nitrogen-containing gases, *Nature*, *346*, 552–554, 1990.
- Lober, J. M., et al., Experimental evaluation of biomass burning emissions: Nitrogen and carbon containing compounds, in *Global Biomass Burning: Atmospheric, Climatic and Biospheric Implications*, pp. 289–304, edited by J. S. Levine, MIT Press, Cambridge, Mass., 1991.
- Mahieu, E., C. P. Rinsland, R. Zander, P. Demoulin, L. Delbouille, and G. Roland, Vertical column abundances of HCN deduced from ground-based infrared solar spectra: Long-term trend and variability, *J. Atmos. Chem.*, *20*, 299–310, 1995.
- Mahieu, E., R. Zander, L. Delbouille, P. Demoulin, G. Roland, and C. Servais, Observed trends in total vertical column abundances of atmospheric gases from IR solar spectra recorded at the Jungfraujoch, *J. Atmos. Chem.*, *28*, 227–243, 1997.
- Palmer, P. I., D. J. Jacob, D. B. Jones, C. Heald, R. Yantosca, J. A. Logan, G. W. Sachse, and D. Streets, Inverting for emissions of carbon monoxide from Asia using aircraft observations over the western Pacific, *J. Geophys. Res.*, *108*(D21), 8828, doi:10.1029/2003JD003397, in press, 2003.
- Rinsland, C. P., et al., Infrared solar spectroscopic measurements of free tropospheric CO, C<sub>2</sub>H<sub>6</sub>, and HCN above Mauna Loa, Hawaii: Seasonal variations and evidence for enhanced emissions from the southeast Asian tropical fires of 1997–1998, *J. Geophys. Res.*, *104*, 18,667–18,680, 1999.
- Rinsland, C. P., E. Mahieu, R. Zander, P. Demoulin, J. Forrer, and B. Buchmann, Free tropospheric CO, C<sub>2</sub>H<sub>6</sub>, and HCN above central Europe: Recent measurements from the Jungfraujoch station including the detection of elevated columns during 1998, *J. Geophys. Res.*, *105*, 24,235–24,249, 2000.
- Rinsland, C. P., A. Goldman, R. Zander, and E. Mahieu, Enhanced tropospheric HCN columns above Kitt Peak during the 1982–1983 and 1997–1998 El Niño warm phases, *J. Quant. Spectrosc. Radiat. Transfer*, *69*, 3–8, 2001.
- Rinsland, C. P., N. B. Jones, B. J. Connor, S. W. Wood, A. Goldman, T. M. Stephen, F. J. Murcray, L. S. Chiou, R. Zander, and E. Mahieu, Multiyear infrared solar spectroscopic measurements of HCN, CO, C<sub>2</sub>H<sub>6</sub>, and C<sub>2</sub>H<sub>2</sub> tropospheric columns above Lauder, New Zealand (45°S latitude), *J. Geophys. Res.*, *107*(D14), 4185, doi:10.1029/2001JD001150, 2002.
- Seiler, W., and P. J. Crutzen, Estimates of gross and net fluxes of carbon between the biosphere and the atmosphere from biomass burning, *Clim. Change*, *2*, 207–247, 1980.
- Singh, H. B., et al., In situ measurements of HCN and CH<sub>3</sub>CN over the Pacific Ocean: Sources, sinks, and budgets, *J. Geophys. Res.*, *108*(D20), 8795, doi:10.1029/2002JD003006, 2003.
- Streets, D., et al., An inventory of gaseous and primary aerosol emissions in Asia in the year 2000, *J. Geophys. Res.*, *108*(D21), 8809, doi:10.1029/2002JD003093, in press, 2003.
- Warneke, C., and J. A. de Gouw, Organic trace gas composition of the marine boundary layer over the northwest Indian Ocean in April 2000, *Atmos. Environ.*, *35*, 5923–5933, 2001.
- Williams, J., et al., An atmospheric chemistry interpretation of mass scans obtained from a Proton Transfer Mass Spectrometer flown over the tropical rainforest of Surinam, *J. Atmos. Chem.*, *38*, 133–166, 2001.
- Wine, P., R. Strekowski, J. Nicovich, M. McKee, G. Chen, and D. Davis, Atmospheric chemistry of HCN, paper PHYS 134 presented at 224rd ACS National Meeting, Am. Chem. Soc., Boston, Mass., 2002.
- Yokelson, R. J., R. Susott, D. E. Ward, J. Reardon, and D. W. T. Griffith, Emissions from smoldering combustion of biomass measured by open-path Fourier transform infrared spectroscopy, *J. Geophys. Res.*, *102*, 18,865–18,877, 1997.
- Yokelson, R. J., et al., Emissions of formaldehyde, acetic acid, methanol, and other trace gases from biomass fires in North Carolina measured by Airborne Fourier Transform Infrared Spectroscopy (AFTIR), *J. Geophys. Res.*, *104*, 30,109–30,125, 1999.
- Yokelson, R. J., I. T. Bertschi, T. J. Christian, P. V. Hobbs, D. E. Ward, and W. M. Hao, Trace gas measurements in nascent, aged, and cloud-processed smoke from African savanna fires by airborne Fourier Transform Infrared Spectroscopy (AFTIR), *J. Geophys. Res.*, *108*(D13), 8478, doi:10.1029/2002JD002322, 2003.
- Zhao, Y., et al., Seasonal variations of HCN over northern Japan measured by ground-based infrared solar spectroscopy, *J. Geophys. Res.*, *27*, 2085–2088, 2000.
- Zhao, Y., et al., Spectroscopic measurements of tropospheric CO, C<sub>2</sub>H<sub>6</sub>, C<sub>2</sub>H<sub>2</sub>, and HCN in northern Japan, *J. Geophys. Res.*, *107*(D8), 4343, doi:10.1029/2001JD000748, 2002.

C. L. Heald, D. J. Jacob, Q. Li, and R. M. Yantosca, Department of Earth and Planetary Sciences, Harvard University, 29 Oxford Street, Pierce Hall Room 107F, Cambridge, MA 02138, USA. (heald@fas.harvard.edu; djj@io.harvard.edu; qli@io.harvard.edu)

M. Koike, Department of Earth and Planetary Science, University of Tokyo, 7-3-1 Hongo Bunkyo-ku, Tokyo, 113-0033, Japan. (koike@eps.s.u-tokyo.ac.jp)

G. W. Sachse, NASA Langley Research Center, Mail Stop 472, 5 North Dryden St., Hampton, VA 23681-2199, USA. (g.w.sachse@larc.nasa.gov)

H. B. Singh, NASA Ames Research Center, Mail Stop 245-5, Moffett Field, CA 94035, USA. (hanwant.b.singh@nasa.gov)

D. G. Streets, Argonne National Laboratory, DIS/900, 9700 South Cass Avenue, Argonne, IL 60439, USA. (dstreets@anl.gov)

Y. Zhao, Department of Mechanical and Aeronautical Engineering, University of California, Davis, One Shields Avenue, Davis, CA 95616, USA. (yzhao@mae.ucdavis.edu)

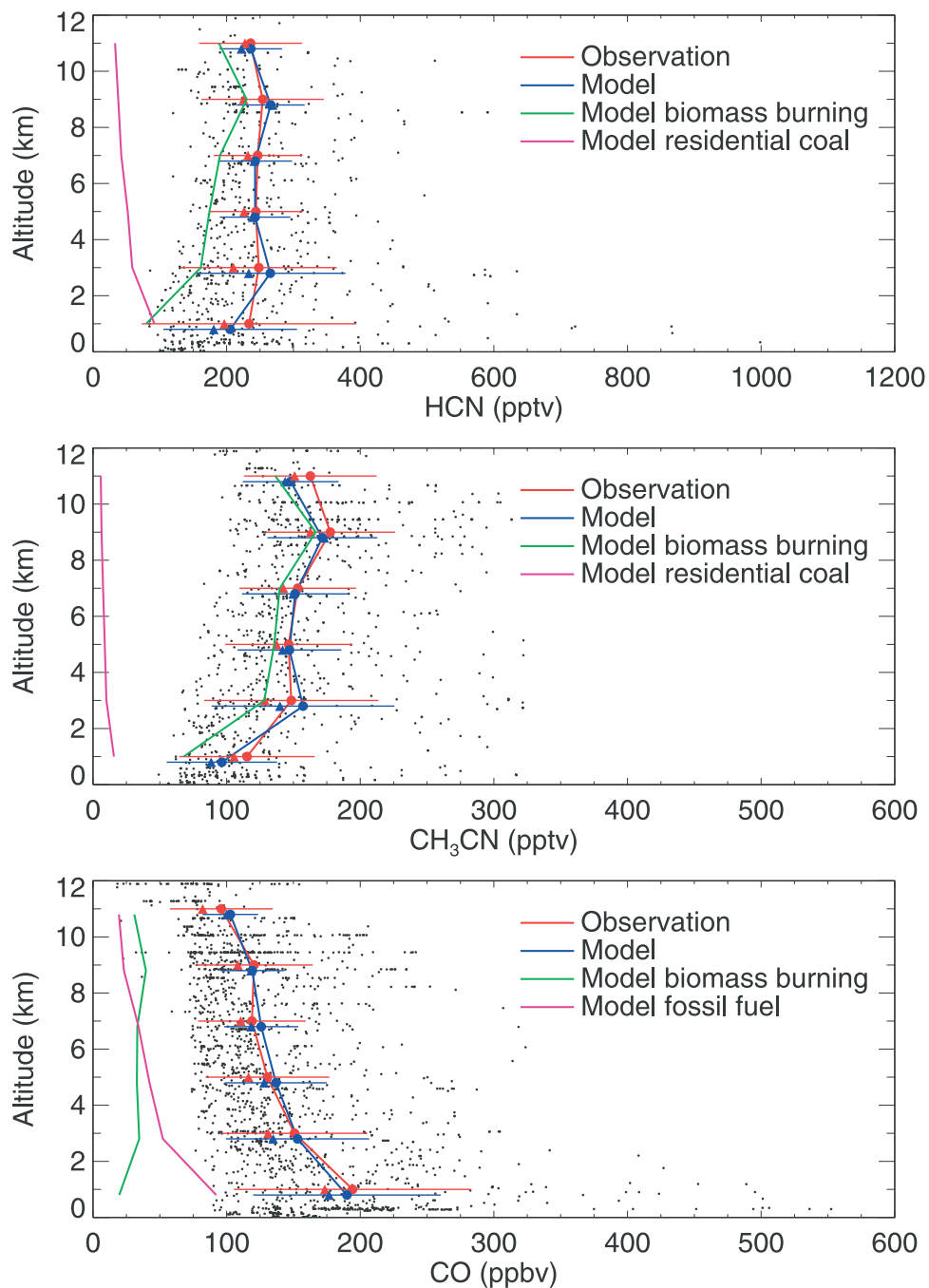


**Figure 1.** Vertical distributions of HCN, CH<sub>3</sub>CN, and CO for the ensemble of TRACE-P data over the NW Pacific (see *Jacob et al.* [2003] for a map of the area covered). Individual observations are shown as dots. Solid circles, triangles, and horizontal bars represent means, medians, and standard deviations, respectively. Model results are shown for the standard simulation and for tagged combustion tracers. Additional sources of CO in the model include biofuel burning and oxidation of methane and biogenic nonmethane hydrocarbons.

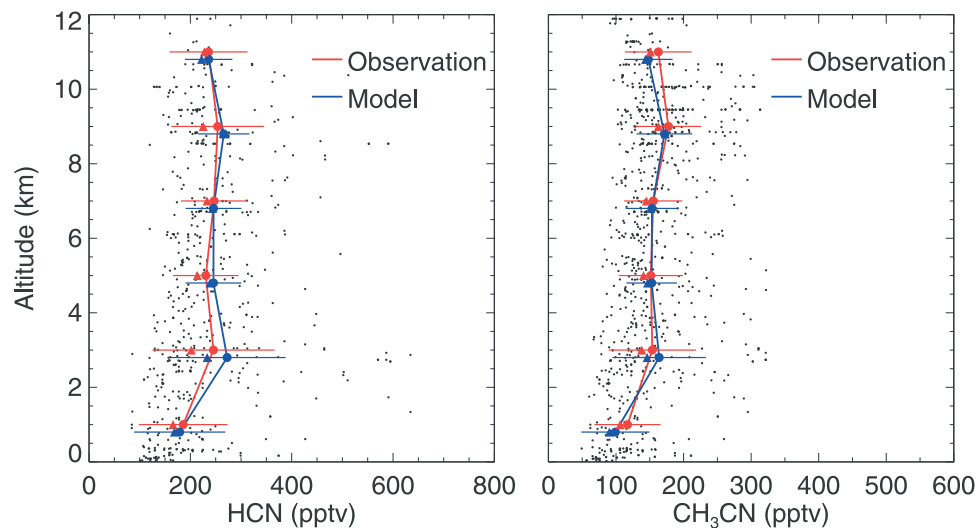


**Figure 2.** Vertical distributions of HCN and CH<sub>3</sub>CN observed in TRACE-P over the North Pacific under background conditions (CO < 120 ppbv and C<sub>2</sub>Cl<sub>4</sub> < 10 pptv). Individual observations are shown as dots. Solid circles, triangles, and horizontal bars represent means, medians, and standard deviations, respectively.

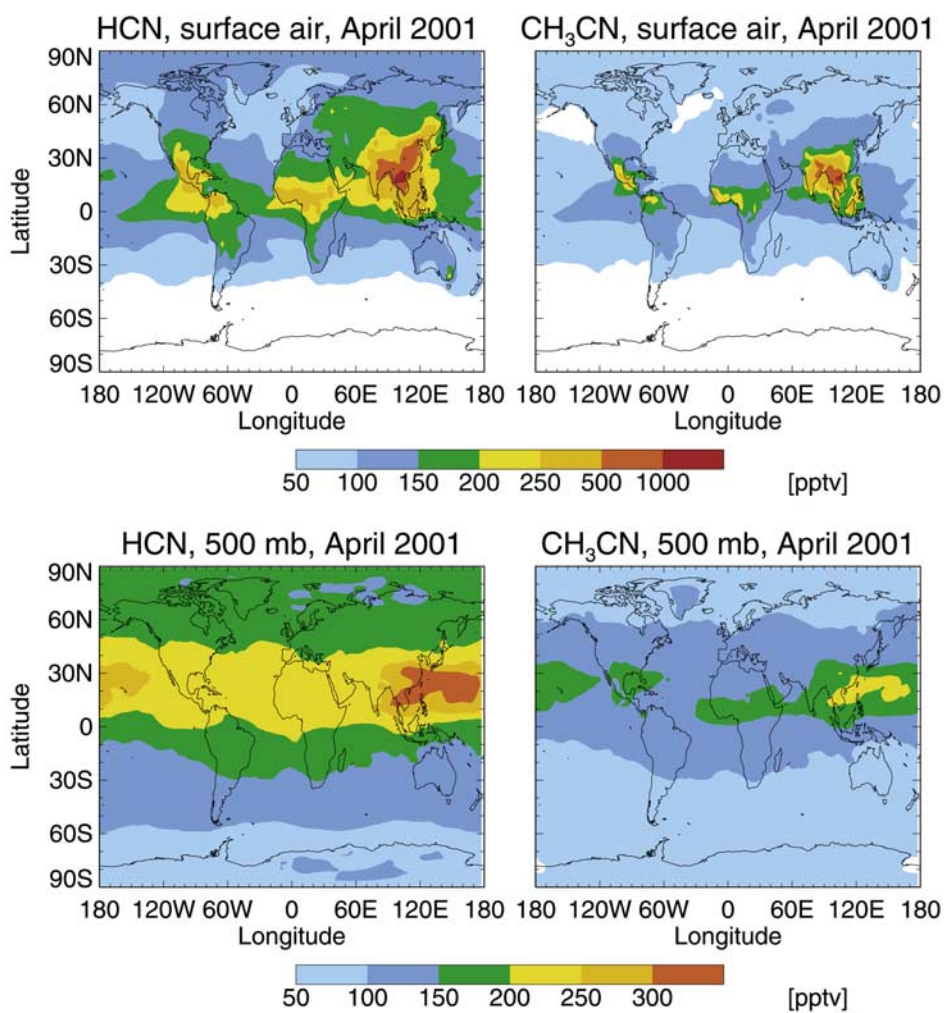


**Figure 13.** Simulated global distributions of HCN and CH<sub>3</sub>CN concentrations in surface air and at 500 hPa for April 2001.